STAFF SUMMARY SHEET

	TO	ACTION	SIGNATURE (Surname), GRADE AND DATE		TO	ACTION	SIGNATURE (Surname), GRADE AND DATE
1	DFP	sig	9 Sep 14 GAUTHIER, LT COL	6			
2	DFER	approve	Solfs, 4032, 9 Sept 14	7			
3	DFP	action		8			
4				9			
5				10			

SURNAME OF ACTION OFFICER AND GRADE	SYMBOL	PHONE	TYPIST'S INITIALS	SUSPENSE DATE
Balthazor, CTR	DFP	333-4231	rlb	15 Sep 14

SUBJECT: Clearance for Material for Public Release — USAFA-DF-PA- 419 — DATE: 9 Sep 14

SUMMARY

1. PURPOSE. To provide security and policy review on the document at Tab 1 prior to release to the public.

2. BACKGROUND.
Authors: Balthazor, R.L. (DFP, 333-4231), McHarg, M.G. (DFP, 333-2460), Enloe, C.L. (DFP, 333-2240), Mueller, B.A.(former DFP cadet), Barnhart, D.J. (DFAS, 333-3315), Hoeffner, Z. (former DFP cadet), Brown, R. (DFAS, 333-4454), Scherliess, L.(Utah State University, 435 797 7189), and Wilhelm, L. T. (former DFP cadet)

Title: Methodology Of Evaluating The Science Benefit Of Various Satellite/Sensor Constellation Orbital Parameters To An Assimilative Data Forecast Model.

Document type: Paper

Description: This is a paper to be submitted to a special issue of the journal Radio Science.

Release Information: General overview good for all audiences

Previous Clearance information: The paper's initial submission has previous been cleared as DFP submission 14010. This submission has been amended/revised to answer points raised by reviewers.

Recommended Distribution Statement: Distribution A, Approved for public release, distribution unlimited.

3. DISCUSSION. This research is funded by AFOSR and the NSF.

4. VIEWS OF OTHERS. N/A

5. RECOMMENDATION. Sign coord block above indicating document is suitable for public release. Suitability is based solely on the document being unclassified, not jeopardizing DoD interests, and accurately portraying official policy.

// signed //

MICHAEL L. GAUTHIER, Lt Col, USAF
Deputy Department Head for Research
Department of Physics

Tabs
1.

1

2 **Methodology of evaluating the science benefit of various satellite/sensor constellation**
3 **orbital parameters to an assimilative data forecast model.**

4 Richard L. Balthazor, Matthew G. McHarg, C. Lon Enloe, Brandon Mueller, David J. Barnhart,
5 Zachary W. Hoeffner, and Robert Brown, United States Air Force Academy, Colorado, USA.

6 Ludger Scherliess, Center for Atmospheric and Space Sciences, Utah State University, Logan,
7 Utah, USA.

8 Lance T. Wilhelm, Air Force Research Laboratory, AFRL/RXCA, Dayton, Ohio, USA

9

10 Corresponding author: R. L. Balthazor, Space Physics and Atmospheric Research Center, HQ
11 USAFA/DFP, 2354 Fairchild Drive, USAF Academy, CO 80840, USA
12 (richard.balthazor@usafa.edu)

13

Key Points

Methodology for evaluating benefit of increasing assimilative data sources

Abstract

A methodology for evaluating the science benefit of adding space weather sensor data from a modest number of small satellites to the Utah State University Global Assimilation of Ionospheric Measurements – Full Physics (GAIM-FP) model is presented. . Three orbital scenarios are presented, two focusing on improved coverage of narrowly specified regions of interest, and one on global coverage of the ionosphere as a whole. An Observing System Simulation Experiment (OSSE) is used to obtain qualitative and quantitative results of the impact of the various orbital scenarios on the ionospheric specifications. A simulated "truth" run of the ionosphere is obtained from a first principles model of the Ionosphere/Plasmasphere model (IPM) and used to generate global simulated Global Positioning Satellite Total Electron Content (GPS-TEC) data as well as in-situ plasma density observations. Initially, only GPS data were assimilated by GAIM-FP and the results of this limited run were compared to the truth run. Next, the simulated in-situ plasma densities corresponding to our three orbital scenarios were assimilated together with the GPS data and the results were compared to both the truth run and the limited GPS-TEC only GAIM-FP run. These model simulations have shown that adding a constellation of small satellites/sensors in addition to global TEC inputs does indeed converge the GAIM-FP model closer to "truth" in the situations described.

35 **Index Terms and Keywords**

36 Ionosphere: Instruments and Techniques

37 Ionosphere: Modeling and Forecasting

38 Radio Science: Instruments and Techniques

39

1. Introduction

In recent years, there have been constructed or proposed space sensor networks [*Anderson* et al, 2002; *Barnhart* et al, 2007a, 2007b; *Barnhart*, 2008; *Barnhart* et al, 2009; *Vladimirova* et al, 2011; *Dyrud* et al, 2013] designed to cover selected orbits in LEO with either:

i) low-cost redundant "disposable" spacecraft-as-sensor platforms of CubeSat 3U size or smaller, or

ii) low-cost low-SWAP (Size, Weight and Power) sensors designed to be placed on as many conventional (ESPA-class or larger) satellites as possible.

The science objective of these missions is to provide a dense set of sensor data parameters to "fill in the gaps" of the relatively sparse coverage afforded by conventional multi-million-dollar missions [*de la Beaujardiere*, 2004] which produce single-point in-situ or remote measurements.

Despite the lower cost of small satellites andlow-SWAP instrumentation, limitations include funding, choice of orbital parameters in launch opportunities, space debris mitigation, and data volume/bandwidth consideration. A key question asked by funders and approvers is still "how many satellites/sensors are enough?" What has become apparent is that there is no generally agreed metric for determining the scientific justification side of this argument, and we propose one methodology to obtain quantitative metrics which may assist in answering that question.

2. Scientific Problem and Background

59 The science problem that we identify for this study is space weather forecasting, particularly
60 forecasting of plasma irregularities ("plasma bubbles") that cause radio and GPS scintillation.
61 Such scintillation can cause loss of GPS lock (less than 50% availability for LPV-200 during
62 severe scintillation [*Seo*, 2010]), loss of communications, and image defocussing in synthetic
63 aperture radar. Forecasting (and nowcasting) ionospheric conditions conducive to plasma bubble
64 formation would seem to require global assimilative models of the ionosphere to provide
65 baseline conditions in the regions of interest.

66 Our ability to specify and forecast ionospheric dynamics and ionospheric weather at low and mid
67 latitudes is strongly limited by our current understanding of the coupling processes in the
68 ionosphere-thermosphere system and the coupling between the high and low latitude regions.
69 Furthermore, only a limited number of observations are available for a specification of
70 ionospheric dynamics and ionospheric weather at these latitudes. As shown by meteorologists
71 and oceanographers, the best specification and weather models are physics-based data
72 assimilation models that combine the observational data with our understanding of the physics of
73 the environment [*Daley*, 1991]. Through simulation experiments these models can also be used
74 to study the sensitivity of the specification accuracy on different arrangements of observation
75 platforms and observation geometries and can provide important information for the planning of
76 future missions. For example, these studies can provide information about the number of
77 spacecraft needed to improve the specification or evaluate the impact of different observation
78 geometries on the accuracy of the specification.

79 **3. Instrument and Satellite Concept**

Previous efforts in flying low-cost space weather instruments have focused on low-impact secondary payloads riding on larger (e.g ESPA-class) satellites. These have advantages, in that the larger satellites tend to be more reliable (through extensive heritage and testing) and have larger link budgets and power margins. However, there are higher integration costs (particularly when co-riding with high-value primary payloads), longer project timescales, and more expensive busses ($10M+). They also provide only a few in-situ measurements for each satellite, and have relatively long delays before resampling the same dataspace.

There have, however, been recent advances in thinking regarding multiple low-cost redundant satellites carrying low-cost sensors.. Such a large constellation has many applications; treaty sentinels, disaster monitoring, magnetospheric observations, solar wind measurements, pollution monitoring and communications research to name but a few. In many of the above cases we currently undersample the data field. We concentrate our approach for this paper on the thermosphere/ionosphere system, ingesting plasma density and temperature data from in-situ measurements into an assimilative model, although the general methodology is applicable to any of the above applications.

With this approach there are a number of suitable instruments with low SWAP that obtain in-situ ionospheric parameters (we restrict ourselves to in-situ measurements for this study, although a similar methodology may be used with remote measurements). The MESA (Miniaturized ElectroStatic Analyzer) instrument [*Enloe* et al, 2002] is a bandpass or high-pass energy filter (in either of two configurations). The instrument thus measures ion or electron spectra (convolved with the instrument response function) from which plasma density and temperature can be derived. MESAs have flown on MISSE-6, MISSE-7 [*Jenkins* et al, 2009], ANDE-2,

FalconSAT-5, STP-H4 and STPSat-3, and are rostered to fly on OTB and other missions. Another instrument of interest is WINCS (Winds Ions Neutrals Composition Suite) and its sister instrument SWATS (Small Wind And Temperature Spectrometer), developed by the Naval Research Laboratory. WINCS and SWATS are sensor suites measuring ion and neutral winds, temperature and composition (http://www.nrl.navy.mil/ssd/branches/7630/SWATS). More generic/traditional Langmuir probes and Retarding Potential Analyzers are also instruments that may with care be integrated into a low SWAP package (although the standoff length of a Langmuir probe may prove to be challenging).

4. GAIM-FP Comparison Methodology

At Utah State University, we have developed two physics-based Kalman-filter data assimilation models for the Earth ionosphere. The two models are the Gauss-Markov Kalman Filter Model (GAIM-GM) and the Full Physics-Based Kalman Filter Model (GAIM-FP) [*Scherliess et al.*, 2006, 2009)]. Both models are part of the Global Assimilation of Ionospheric Measurements (GAIM) project (*Schunk et al.* 2004) . Some of the data that we have previously assimilated in our data assimilation models include in-situ electron density measurements from DMSP satellites, bottomside electron density profiles from ionosondes, GPS-TEC data from a network of up to 1000 ground stations, ultraviolet (UV) radiances from the SSUSI (Special Sensor Ultraviolet Spectrographic Imager), SSULI (Special Sensor Ultraviolet Limb Imager), and LORAAS (Low Resolution Airglow and Aurora Spectrograph) instruments, and radio occultation data from CHAMP (Challenging Minisatellite Payload) andSAC-C (Satellite de Aplicaciones Cientificas-C) (Hajj et al, 2004)IOX (Ionospheric Occultation Experiment) (*Straus*

124 *et al*, 2003), and the COSMIC (Constellation Observing System for Meteorology, Ionosphere
125 and Climate) (*Rocken et al*, 2000) satellite.

126 The Full Physics-Based Kalman filter model is based on an ensemble Kalman filter approach
127 (Evensen, 2003) and rigorously evolves the ionosphere and plasmasphere electron density field
128 and its associated errors using a physics-based Ionosphere-Plasmasphere model (IPM) [*Schunk* et
129 *al.*, 2004, 2005; *Scherliess et al.*, 2004]. The IPM is based on a numerical solution of the ion and
130 electron continuity and momentum equations and covers the low and mid-latitudes from 90 to
131 30,000 km altitude. In its current version, the model excludes geomagnetic latitudes poleward of
132 $\approx \pm 60°$ geomagnetic latitude due to the vastly different physical processes that govern the high-
133 latitude regions, e.g. convection electric fields, particle precipitation, etc. The Full Physics-Based
134 data assimilation model provides specifications on a spatial grid that can be global, regional, or
135 local and its output includes the 3-dimensional electron and ion (NO^+, O_2^+, N_2^+, O^+, H^+, He^+)
136 density distributions from 90 km to geosynchronous altitude (30,000 km). In addition, the model
137 provides the global distribution of the ionospheric drivers (electric field, neutral wind, and
138 composition) that are consistent with the ionospheric observations. It is important to note that
139 the estimation of the ionospheric drivers is an integral part of our ensemble Kalman filter and is
140 achieved by using the internal physics-based model sensitivities to the various driving forces. In
141 this procedure, the ionospheric data are used to adjust the plasma densities and its drivers so that
142 a consistency between the observations (within their errors) and the physical model is achieved.
143 As a result the assimilation procedure produces the optimal model-data combination of the
144 ionosphere-plasmasphere system with its self-consistent drivers (electric fields and neutral winds
145 and composition) [*Scherliess et al.*, 2009, 2011].

146 **5.1 Kalman Filter Simulations**

147 The Full Physics-Based data assimilation model was designed to specify ionospheric weather,
148 but the model can also be used to study the sensitivity of the specification accuracy on different
149 arrangements of observation platforms and observation geometries and can provide important
150 information for the planning of future missions [*Atlas,* 1997; *Atlas et al.,* 1985]. For the current
151 study this latter mode has been used and simulation experiments have been performed. In this
152 mode the model uses a Data Simulation System Experiment (OSSE) using two different
153 synthetic (model-generated) data types: slant TEC from ground-based GPS stations and in-situ
154 plasma density measurements obtained from electrostatic analyzers (ESA) onboard of a
155 constellation of small satellites. Figure 1 shows the geographical distribution of ground GPS-
156 TEC stations chosen for this study. In the OSSE, the simulated weather (true) time-dependent ion
157 and electron density distributions are generated by using again the IPM model. For this study we
158 have used two geomagnetically quiet days, 2010 day 73 and 74 (March $14^{th}/15^{th}$) where Kp~1
159 throughout the two days. These two days were chosen to assist in another study comparing
160 actual MESA data from the MISSE7 experiment on the ISS with the GAIM predictions; that
161 work is outside the scope of this paper. For the simulations we varied the equatorial vertical drift
162 and horizontal neutral winds by superposing on the climatology values a random component.
163 Note that neither the climatological values nor the random components are known to the
164 ensemble Kalman filter part. The synthetic data were then generated by probing the 3-D, time-
165 dependent electron density distribution for the weather (true) simulation exactly the same way
166 the real instruments probe the real ionosphere. For the GPS receivers, slant TEC values were
167 generated only for elevation angles greater than 15°. For the in-situ electron densities synthetic
168 observations were generated in 10-sec increments. When the synthetic data were generated, noise

169 was added to each ''measurement'' in order to mimic a real observation. A 5 TEC unit (TECU)
170 level of noise was added to all simulated TEC measurements and a 10% uncertainty to the
171 simulated in-situ measurements. . It should be noted that the 10 second resolution of the
172 observations is not intended to capture variations that occur on this small time step, but instead to
173 capture spatial variations of the order of about 100-150 km around the latitudinal resolution of
174 the model. 10 seconds is also the nominal cadence of data-taking in the IMESA instrument
175 (although it is capable of running as fast as 2Hz). The satellites traverse a distance of about 70
176 km in 10 seconds, which provides about two observations per latitude grid cell. The model time
177 step of 15 minutes was chosen to capture typical variations in the ionospheric F-region where the
178 characteristic timescales are of the order of tens of minutes.

179

180 The ensemble Kalman filter assimilation procedure was implemented as follows. At 0000 UT on
181 day 2010/073 the plasma distribution obtained from the "truth" run (the IPM run with the
182 modified climatological neutral wind and equatorial electric field input) was taken to be the
183 initial distribution at the start of the assimilation. Every 15 min, the evolving weather simulation
184 was probed to obtain the two synthetic data types (with noise) as described above. At these time
185 marks the ensemble of ionosphere/plasmasphere model runs was also integrated forward in time,
186 and the model error covariance matrix was determined [Scherliess et al., 2007]. Using the new
187 data and the new error matrix, the ensemble Kalman filter reconstructed an updated estimate of
188 the plasma distribution and its drivers. The new drift and wind velocities were fed back into the
189 IPM and the assimilation was repeated at the next 15 min time mark. As time advanced, the
190 ensemble Kalman filter produced a 3-D, time-dependent, plasma distribution that got closer and

191 closer to the 'true' plasma distribution associated with our weather simulation

192 To qualitatively and quantitatively assess the impact of the MESA observations on the plasma
193 specifications four ensemble Kalman filter simulations were performed. Initially, the GAIM-FP
194 model assimilated only the simulated global TEC data to obtain a specification of the plasma
195 density for the two days. This model simulation is referred to as the "ionospheric specification"
196 and may be compared with the "truth" measurement to determine the accuracy of the data
197 assimilation model.

198 Next, the synthetic MESA "observation", including an observational uncertainty, were
199 assimilated together with the synthetic global TEC data to simulate data-taking from satellite
200 constellations that did not, in reality, exist at that particular time. The simulated observations
201 were taken along satellite tracks for three different orbital scenarios at 10 second simulated
202 cadenceThe orbital scenarios were chosen to give both low-cost (single launch) rapid re-
203 coverage of a localized area, and higher-cost (multiple launches) global coverage. We also
204 wished to investigate effect of varying the altitude of the satellites on the sensitivity of the
205 specification. Accordingly, the three orbital scenarios chosen were as follows:

206 Scenario A: Ten satellites in a circular 500 km polar orbit (90° inclination) at longitude
207 161.25° E (the Pacific sector, where GPS TEC ground stations are relatively sparse compared
208 to over continental land masses). Small (deliberate) variations in the satellite surface
209 treatment will lead to small variations in satellite drag, causing the satellites to distribute
210 themselves along the orbital path until they are spread evenly along the orbit. This represents
211 the "string of pearls" configuration for a single launch/deployment.

212 Scenario B: As scenario A, but at a 350 km altitude.

213 Scenario C: A 25/5/1 Walker constellation at 510 km altitude and 60° inclination. The
214 Walker constellation notation of *t/p/f* designates *t* satellites arranged over *p* evenly spaced
215 orbital planes (circular orbits) with *f* relative spacing between satellites in adjacent planes.
216 Thus, a 25/5/1 constellation has 25 satellites, five satellites per orbital plane. We have picked
217 a nominal relative spacing in this instance. This would generally require five launch vehicles,
218 each deploying five satellites, with each group deploying into the string of pearls
219 configuration after some weeks. Figure 2 shows (lower panel) Ne at 510 km, and (upper
220 panel) the ground tracks of a 25/5/1 Walker constellation with the color scale along each
221 ground track demonstrating the sampling of Ne.

222 For each of the three orbital scenarios the GAIM-FP model was used together with the global
223 TEC inputs and the MESA "observation" to obtain another set of specifications of the same day.
224 These model simulations are referred to as the "improved ionospheric specification", and may be
225 compared to the original "ionospheric specification" (without any MESA data inputs) and the
226 original "truth" model run.

227 **5. Results**

228 For Scenarios A and B, we have examined a vertical slice of the ionosphere from 100 km to 600
229 km along the 161. 25° E line of longitude of the orbital plane, stretching from 60° N to 60° S.
230 (Plots are plotted to the poles, but the GAIM model used only extends to +/-60° magnetic
231 latitude). Figure 3 shows the deviation from "truth" in units of ΔNe (cm^{-3}) for three simulation
232 runs: "ionospheric specification" using only GPS-TEC inputs to the assimilative forecast model

233 (left panel), "improved ionospheric specification" using GPS-TEC inputs plus inputs from
234 satellites in scenario A (center panel) (satellites at 500 km), and "improved ionospheric
235 specification" using GPS-TEC inputs plus inputs from satellites in scenario B (right panel)
236 (satellites at 350 km).

237 A visual inspection of the data shows that utilizing inputs from a modest constellation of ten
238 satellites at either of two altitudes shows a distinct improvement to the "improved ionospheric
239 specification" (ΔNe converges towards zero). What is perhaps remarkable is that the
240 improvement is distinct at most latitudes and can be seen at all altitudes and not just at the orbital
241 altitude. The apparent propagation of information to other altitude regimes is a manifestation of
242 the strong correlation of electron density variations along geomagnetic field lines. These
243 correlations are part of the ensemble Kalman filter and automatically calculated using the
244 ensemble of physics-based model runs.This indicates that the useful life of such a constellation,
245 as orbital drag decays the orbit from the initial insertion, will be extended through the life of the
246 mission (months to years for higher initial orbital insertions), rather than losing their use after
247 initial orbital decay.

248 Scenario C allows inspection of global (latitude-longitude) coverage. We have elected to use
249 hmF2 as a proxy for our knowledge of the ionosphere (remembering that although the satellites
250 in Scenario C are at 500 km, the earlier results indicate that information is apparently
251 propagating vertically (owing to the correlation of electron density along magnetic field lines in
252 the ensemble Kalman filter) allowing us to inspect the ionosphere and the improvement to the
253 plasma specifications at any altitude). We inspect hmF2 at an arbitrary time of 1600 GMT on
254 day 2. Figure 4 shows hmF2 from the "truth" model (plotted to the latitude limits of the model)

255 at the selected time. Figure 5 shows hmF2 obtained from the "ionospheric specification" model
256 using only GPS-TEC inputs to the model. A visual inspection shows that there are deviations
257 from "truth". In particular, the height enhancement over the Japanese sector is not found; there
258 is an erroneous equatorial plume forecast over the Indonesian sector; and the pronounced
259 equatorial anomaly over the South American sector is not seen in the data assimilation results for
260 this limited model run.

261 Figure 6 shows hmF2 obtained from the "improved ionospheric specification", utilizing GPS-
262 TEC inputs plus simulated data from the MESA instruments in the Walker constellation of
263 scenario C. Inspection shows that the three features mentioned above, reproduced poorly by the
264 "ionospheric specification", are present in the "improved ionospheric specification".

265 The previous examples are qualitative. There are many quantitative metrics that can be used to
266 quantify the improvement, and we have arbitrarily selected two metrics, the RMS deviation
267 (global sum) and the Skill Score (global sum). The RMS deviation, summed over all latitude-
268 longitude points at each hmF2 altitude, is given by the sum of the squares of the deviations from
269 truth divided by the number of observations and is measured in km (equation 1). Improved
270 modeling will reduce the RMS deviation towards zero.

271 The Skill Score is a measure of improvement of one model over another and is unitless, ranging
272 from –infinity to +1. If the second model is perfect the Skill Score tends to +1, and if the second
273 model predicts no better than random chance the Skill Score tends towards 0 (equation 2).

274 $$RMS = \sqrt{\frac{\sum(Truth - Obs)^2}{N}} \qquad (1)$$

Formatted: Font: Times New Roman, Not Italic

$$Skill\ Score = 1 - \frac{\sum(Truth - (GPS+IMESA))^2}{\sum(Truth - GPS\ only)^2} \quad (2)$$

Figure 7 shows the RMS deviation from truth global sum over a 24-hour period on 2010 day 073. With the "ionospheric specification" (GPS-TEC only), the RMS deviation from truth varies between 25 km and 100 km over the course of the 24 hours. It is interesting to note the variation over time, and we suggest that this is due a function of daytime and nighttime regions being densely or less densely populated with GPS-TEC ground stations, as the sun moves from the Pacific sector (less densely populated with GPS-TEC ground stations) to the American and European sectors (more densely populated). With the "improved ionospheric specification" (GPS-TEC plus simulated MESA data from scenario C), which of course are agnostic to day-night variations, the RMS deviation global sum improves to around 10 km over the course of the day.

The Skill Score comparison of the two model runs is shown in Figure 8. Again we see a pronounced diurnal response, with the "improved ionospheric specification" performing extremely well in the 0000 UT to 0600 UT, and 1800 UT to 2359 UT timeframes, and marginally less well between those timeframes. However, with the Skill Score minimum being ~0.75, we can conclude that overall there is a marked improvement to our forecast model with 25 MESAs in orbital scenario C.

We recognize that the results obtained from these metrics can depend on other parameters such as geomagnetic activity, but such an investigation is outside the bounds of this paper.

6. Conclusions

295 We have proposed using a simple sensor that measures ion and electron energy spectra, from
296 which plasma density and temperature can be derived, in a low-cost mission of small
297 satellites/sensors. A full physics ionospheric model has been utilized to derive "truth" data. The
298 GAIM-FP forecast model has then been run both without and with simulated sensor data inputs.
299 Our model simulations have shown that adding a constellation of small satellites/sensors in
300 addition to global TEC inputs converges the GAIM-FP model closer to "truth" in the situations
301 we describe. For a real-life mission for which a launch has not been imposed, a desired
302 improvement metric may be selected and thus orbital parameters can be fine-tuned to optimize
303 the model improvement for the metric of interest.. What is particularly interesting is that the
304 model is improved over a range of altitudes, not just at and around the satellite/sensor altitude,
305 emphasizing the coupled nature of both the model and reality, (and in particular here, the strong
306 correlation of electron density along geomagnetic field lines in both the model and reality). Put
307 another way, knowledge at one location leads to improved knowledge at other locations.

308 However, what has become apparent is the challenge to develop a generally agreed metric or set
309 of metrics to measure the scientific and operational benefit to assimilative models from the use
310 of multiple small satellite/sensor inputs.

311 **7. Acknowledgements**

312 The authors wish to thank the Air Force Office of Scientific Research for their support.

313 The work at Utah State University was partially supported by NSF grant AGS-1329544.

314 The GAIM-FP data is publically available on request from USU, POC Ludger Scherliess,
315 ludger.scherliess@usu.edu

8. References

Anderson, B. J., Takahashi, K., Kamei, T., Waters, C. L., & Toth, B. A. (2002). Birkeland current system key parameters derived from Iridium observations: Method and initial validation results. *Journal of Geophysical Research: Space Physics (1978–2012)*, *107*(A6), SMP-11.

Atlas, Robert (1997) Atmospheric observations and experiments to assess their usefulness in data assimilation. JMSJ, Vol. 75, pp. 111-130.

Atlas, R., E. Kalnay, J. Susskind, W. E. Baker and M. Halem (1985): Simulation studies of the impact of future observing systems on weather prediction. Proc. Seventh Conf. on NWP. 145-151.

Barnhart, D. J., T. Vladimirova, M. N. Sweeting, R. L. Balthazor, C. L. Enloe, L. H. Krause, T. J. Lawrence, M. G. Mcharg, J. C. Lyke, J. J. White, and A. M. Baker (2007), Enabling Space Sensor Networks with PCBSat, AIAA Paper SSC07-IV-4

Barnhart, D. J., T. Vladimirova, and M. N. Sweeting, (2007), Very Small Satellite Design for Distributed Space Missions, Journal of Spacecraft and Rockets, Vol. 44, No. 6, pp. 1294-1306.

Barnhart, D. J. (2008), Very Small Satellites Design for Space Sensor Networks, Ph.D. Thesis, Univ. of Surrey, Guildford, England, U.K., http://handle.dtic.mil/100.2/ADA486188

Barnhart, D.J, T. Vladimirova and M.N. Sweeting (2009), Satellite Miniaturization Techniques for Space Sensor Networks, Journal of Spacecraft and Rockets, Vol 46, No. 2, doi 10.2514/1.41639

336 Daley, R. (1991), Atmospheric Data Analysis, Cambridge University Press, Cambridge, UK

337 De la Beaujardiere, O. (2004), C/NOFS: a Mission to Forecast Scintillations, Journal of
338 Atmospheric and Solar-Terrestrial Physics, Vol. 66, No. 17, pp. 1573–1591.

339

340 Dyrud, L. P., Fentzke, J. T., Cahoy, K., Murphy, S., Wiscombe, W., Fish, C., Gunter, B., Bishop,
341 R., Bust, G., Erlandson, R., Bauer, B., & Gupta, O. (2012), GEOScan: a geoscience facility from
342 space. In *SPIE Defense, Security, and Sensing* (pp. 83850V-83850V). International Society for
343 Optics and Photonics.

344

345 Enloe, C. L., J. Lloyd, S. Meassick, C. Chan, J. O. McGarity, A. Huber, and P. Hartnett (1995),
346 Compact Thermal Ion Detector for Space and Laboratory Applications, Review of Scientific
347 Instruments 66.8, 4174-719Enloe, C. L., L. Habash Krause, R. K. Haaland, T. T. Patterson, C. E.
348 Richardson, C. C. Lazidis, and R. G. Whiting (2002), Miniaturized electrostatic analyzer
349 manufactured using photolithographic etching, Review of Scientific Instruments 74:3, DOI:
350 10.1063/1.1540715

351

352 Evensen, G. (2003), The Ensemble Kalman Filter: Theoretical Formulation and Practical
353 Implementation, *Ocean Dynamics*, *53*, 343–367, DOI 10.1007/s10236-003-0036-9.

354 Hajj, G. A., C. O. Ao, B. A. Iijima, D. Kuang, E. R. Kursinski, A. J. Mannucci, T. K. Meehan, L.
355 J. Romans, M. de la Torre Juarez, and T. P. Yunck (2004), CHAMP and SAC-C atmospheric
356 occultation results and intercomparisons, *J. Geophys. Res.*, *109*, *D06109*,
357 *doi:*10.1029/2003JD003909.

358 Kalman, A., A. Reif, D. Berkenstock, J. Mann and J. Cutler (2008), MISC - A Novel Approach
359 to Low-Cost Imaging Satellites, Proceedings of the 22nd Annual Conference On Small Satellites

360 Jenkins, P., R.J. Walters, M. J. Krasowski, J. J. Chapman, P. G. Ballard, J. A. Vasquez, D. R.
361 Mahoney, S. N. LaCava, W. R. Braun, N. F. Prokop, J. M. Flatico, L. C. Greer, K. B. Gibson,
362 W.H. Kinard, and H. G. Pippin (2009), MISSE-7: Building a Permanent Environmental Testbed
363 for the International Space Station, Proceedings of the 9th International Space Conference
364 Protection of Materials and Structures From Space Environment, Toronto, Canada, 19-23 May
365 2008, Ed. J.I. Kleiman, AIP Conference Proceedings 1087, pp. 273-276

366 Kalman, A. Reif, and J. Martin (2013), MISC 3 – The next generation of 3U CubeSats,
367 Proceedings of the CubeSat Developers Summer Workshop

368 Rocken, C., Y.H. You, W.S. Schreiner, D. Hunt, S. Sokolovskiy, and C. McCormick (2000),
369 COSMIC system description, *Terrestrial Atmospheric and Oceanic Sciences, 11*, 1, pp 21-52

370 Scherliess, L., R.W. Schunk, J.J. Sojka, and D. Thompson (2004), Development of a Physics-
371 Based Reduced State Kalman Filter for the Ionosphere, *Radio Sci.*, *39*, RS1S04,
372 doi:10.1029/2002RS002797.

373 Scherliess, L. D. Thompson, R.W. Schunk, and J.J. Sojka (2006), Ionospheric/thermospheric
374 variability at middle latitudes obtained from the global assimilation of ionospheric measurements
375 (GAIM) model, *Eos Trans. AGU,* 87(52), Fall Meet. Suppl., Abstract SA12A-03.

376 Scherliess, L., D.C. Thompson, and R.W. Schunk (2009), Ionospheric dynamics and drivers
377 obtained from a physics-based data assimilation model, Radio Science, 44, RS0A32, doi:
378 10.1029/2008RS004068.

379 Scherliess, L., D.C. Thompson, and R.W. Schunk (2011), Data assimilation models: A 'new'
380 tool for ionosphere science and applications, in *The Dynamic Magnetosphere*, Springer, doi
381 10.1007/978-94-007-0501-2_18

382 Schunk, R.W., L. Scherliess, J.J. Sojka, and D. Thompson (2004), Global Assimilation of
383 Ionospheric Measurements (GAIM), *Radio Sci*, *39*, RS1S02, doi:10.1029/2002RS002794.

384 Schunk, R.W., L. Scherliess, J.J. Sojka, D. Thompson, and L. Zhu (2005), Ionospheric Weather
385 Forecasting on the Horizon, *Space Weather*, 3, S08007, doi:10.1029/2004SW000138.

386 Seo, J (2010), Overcoming Ionospheric Scintillation for Worldwide GPS Aviation, PhD thesis,
387 Stanford University, CA

388 Straus, P. R., P. C. Anderson, and J. E. Danaher (2003), GPS occultation sensor observations of
389 ionospheric scintillation, Geophys. Res. Lett., 30, 1436, doi:10.1029/2002GL016503, 8.

390 Vladimirova, T., N. P. Bannister, J. Fothergill, G. W. Fraser, M. Lester, D. M. Wright, M. J.
391 Pont, D. J. Barnhart, O. Emam (2011), CubeSat Mission for Space Weather Monitoring,
392 Proceedings of 11th Australian Space Science Conference, ASSC'11, Canberra, Australia.

393

394 **Figures**

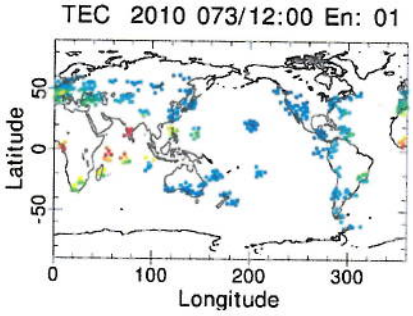

395

396 **Figure 1: Geographical distribution of ground-based GPS-TEC stations chosen for this**
397 **study. The figure shows the 300 km pierce points of observations at the given time**
398 **(2010/073 1200 UT), and the color scale depicts vertical TEC with blue indicating low TEC**
399 **and red indicating high TEC.**

400

401

402 .

403

404

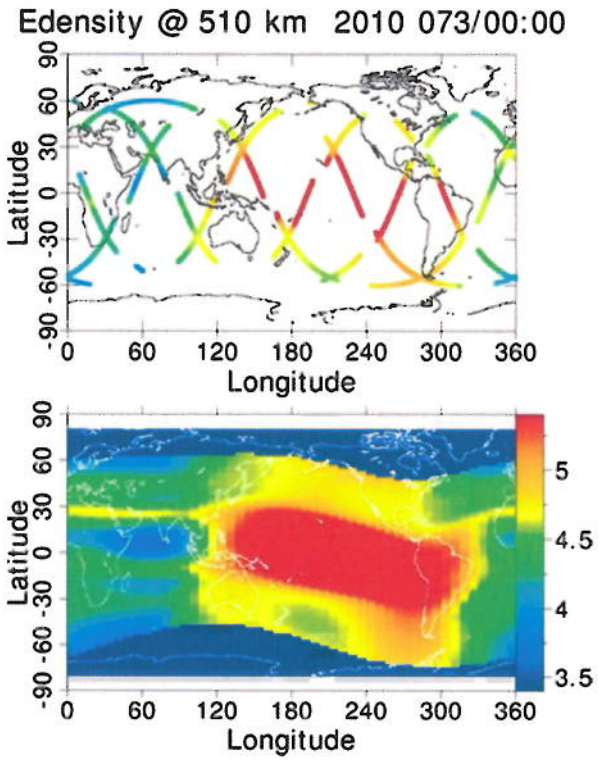

405

406 **Figure 2: (upper panel) 25/5/1 Walker constellation ground tracks showing sampling of Ne**

407 **from "truth" model run , and (lower panel) snapshot of Ne obtained from an "improved**

408 **ionospheric specification" forecast model (GPS-TEC and sampled MESA data)**

409

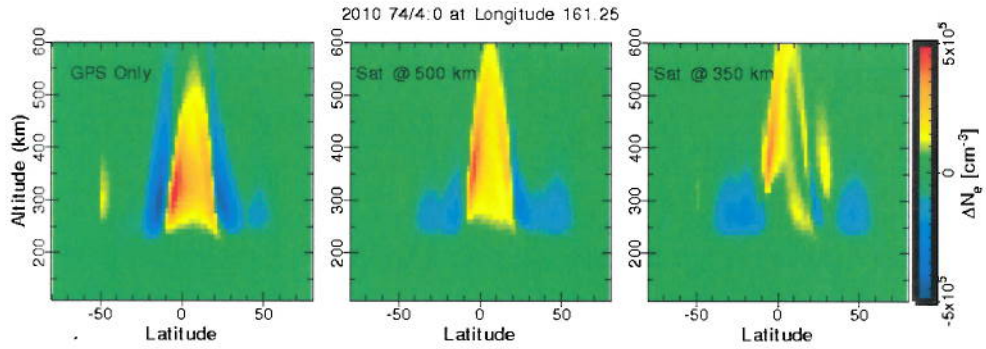

410

411 **Figure 3: Model deviations from "truth" run for scenarios A and B, over the altitude-**
412 **latitude slice at longitude 161.25°E. Changes in Ne are denoted by variations in the color**
413 **scale from green (no deviation).**

414

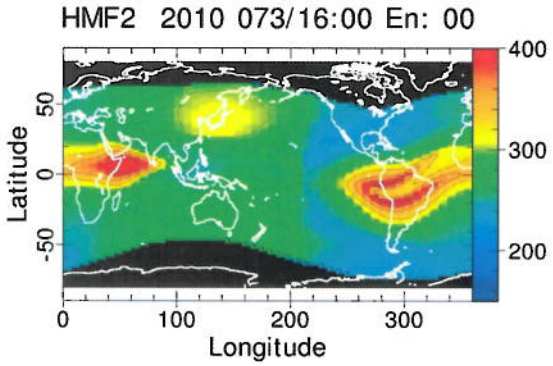

415

416 **Figure 4: "Truth" model of hmF2**

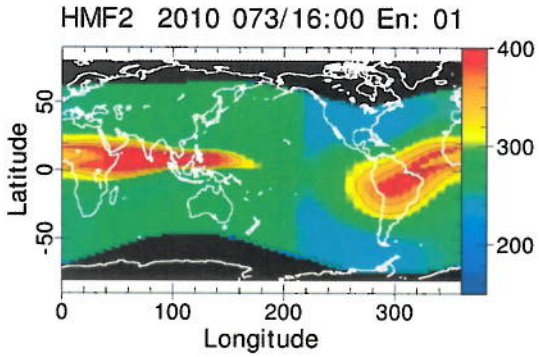

417

418 **Figure 5: hmF2 "ionospheric specification" model of hmF2 using only GPS-TEC inputs to**

419 **the GAIM-FP model**

420

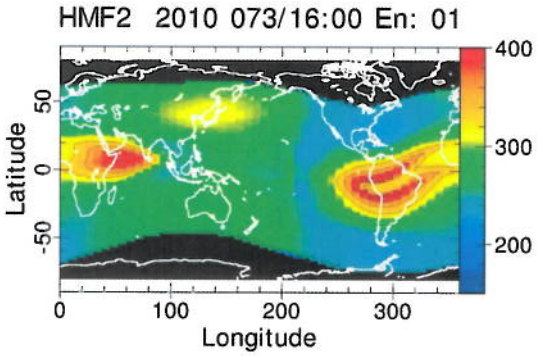

421

422 **Figure 6: hmF2 "improved ionospheric specification" model of hmF2 using GPS-TEC and**

423 **in-situ MESA data**

424

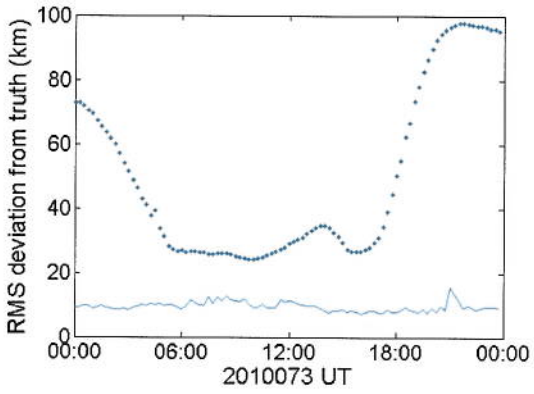

425

426 **Figure 7: RMS deviation of hmF2 prediction (global sum). The upper (dotted) line shows**
427 **predictions from the "ionospheric specification" (GPS-TEC only); the lower (solid) plot**
428 **shows the predictions for "improved ionospheric specification" (GPS-TEC and MESA**
429 **inputs).**

430

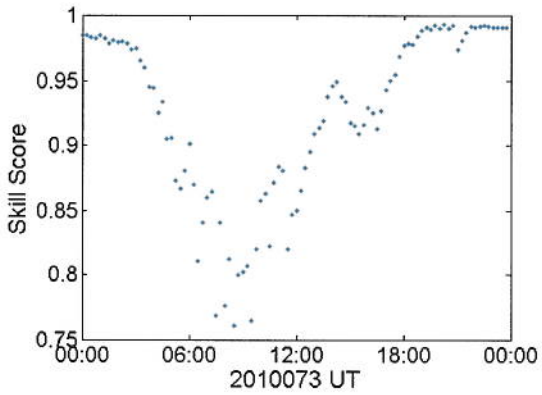

431

432 **Figure 8: Skill Score of hmF2 prediction, comparing "improved ionospheric specification"**

433 **to "ionospheric specification".**

434